Tellus (1995), 47B, 93–102
Printed in Belgium – all rights reserved

TELLUS
ISSN 0280–6509

Distribution of the CO_2 partial pressure in the Atlantic ocean between Iceland and the Antarctic peninsula

By B. SCHNEIDER[1]* and J. MORLANG[2], [1]*Institute for Baltic Sea Research, Seestr. 15, 18119 Rostock-Warnemünde, Germany*; [2]*Institute for Marine Research, Düsternbrooker Weg 20, 24105 Kiel, Germany*

(Manuscript received 3 February 1994; in final form 14 October 1994)

ABSTRACT

CO_2 partial pressure of surface water, $(pCO_2)_{sw}$, was measured continuously during two cruises in the Atlantic Ocean in November/December 1991 and May 1992. A $(pCO_2)_{sw}$ profile between Iceland and the Antarctic Peninsula is obtained which demonstrates that along the investigated transect the Atlantic Ocean is largely a potential sink for atmospheric CO_2, especially at high latitudes, where partial pressure differences of $-80\,\mu$atm to $-100\,\mu$ atm are observed. A significant potential source region exists only between the equator and 10° S with a maximum ΔpCO_2 of 35 μatm. An attempt is made to identify the processes that control the $(pCO_2)_{sw}$ distribution pattern. The investigations at latitudes >40° in both hemispheres were performed during spring and correlations between $(pCO_2)_{sw}$ and chlorophyll *a* contents indicate that biological production mainly controls the distribution of $(pCO_2)_{sw}$. At lower latitudes, $(pCO_2)_{sw}$ is mainly related to temperature and salinity, but also an upwelling effect could be identified close to the equator.

1. Introduction

Anthropogenic CO_2 emissions have imposed strong perturbations to the global carbon cycle. During the past 200 years, the atmospheric CO_2 content increased by about 30% from 280 ppm in pre-industrial times to a present value of about 360 ppm. Predictions of the future development of atmospheric CO_2 require knowledge about the response of the ocean to anthropogenic CO_2 fluxes.

During 1980–1989, about 7.0 GtC CO_2 were annually released to the atmosphere by combustion of fossil fuel and other human activities (Watson et al., 1992; Sarmiento and Sundquist, 1992). As 3.2 GtC/y stay in the atmosphere, a sink for the remaining 3.8 GtC/y must exist. Both the ocean and the terrestrial biosphere have the potential to store CO_2. Different approaches have been used to recognize the oceanic uptake of anthropogenic CO_2 on the background of the natural CO_2 exchange between the ocean and the atmosphere: box diffusion models, ocean circulation models, atmospheric circulation models and CO_2 flux balances on the basis of measurements. The results of these methods differ between 1.5 and 2.5 GtC/y (Keeling et al., 1989; Bacastow and Maier-Reimer, 1990; Tans et al., 1990; Sarmiento and Sundquist, 1992; Orr, 1993).

The flux of CO_2 at the sea surface is thermodynamically driven by the difference between the CO_2 partial pressure of seawater and in the atmosphere $(\Delta pCO_2 = (pCO_2)_{sw} - (pCO_2)_{atm})$. The purpose of our investigations is to enhance the spatial and seasonal data coverage for $(pCO_2)_{sw}$ and thus to contribute to refined CO_2 flux calculations and to realistic global flux balances by which the anthropogenic CO_2 uptake by the ocean may be estimated. We will not present a regional or global CO_2 budget because the ΔpCO_2 data base is still too modest in the light of the strong variability of $(pCO_2)_{sw}$. The data will rather be used to reveal the interplay of the different processes which

* Corresponding author.

determine the distribution pattern of $(pCO_2)_{sw}$ in surface waters: changes in temperature and salinity, exchange with the atmosphere, biological activity and mixing with subsurface water.

2. Experimental

The CO_2 partial pressure of surface water was investigated during two cruises in the Atlantic Ocean. Data for 62°S–40°N were collected onboard R. V. POLARSTERN during the expedition ANTX/1 in November/December 1991 and for 40°N–63°N during the expedition M21 with R. V. METEOR in May 1992 (Fig. 1).

Surface $(pCO_2)_{sw}$ was measured continuously using an equilibration/IR detection system as described previously by Schneider et al. (1992). Seawater was pumped from a depth of about 10 m and temperature/salinity at the seawater inlet were recorded. Changes in temperature during pumping did not exceed 1°C and its effect on $(pCO_2)_{sw}$ was corrected using the formula of Gordon and Jones (1973). Application of alternative temperature corrections as suggested by Weiss et al. (1982), Copin-Montegut (1988), Takahashi et al. (1993) and others lead to only slightly differing results. For example, using a temperature coefficient 0.0423 l/°C as proposed by Takahashi et al. (1993) gives a difference in the corrected pCO_2(sw) of $-0.15\,\mu$atm at $250\,\mu$atm and of $+0.04\,\mu$atm at $400\,\mu$atm for a temperature change of 1°C. These deviations are neglectable. Measurements of $(pCO_2)_{sw}$ were interrupted each 12 h for the calibration of the IR analyzer and for maintenance of the measurement system. The determination of CO_2 in air was performed sporadically after calibration of the system. The precision of the method was estimated to be 1–2 μatm for $(pCO_2)_{sw}$ and 0.5 μatm for $(pCO_2)_{atm}$.

Between 40°S and 40°N total carbonate, TCO_2, was measured each 60 nautical miles in surface water. At a few stations also the vertical distribution of TCO_2 was determined. Only the data from two stations (Fig. 1) are relevant for this paper and are discussed. The analysis of TCO_2 was performed by a coulometric method according to Johnson et al. (1987) and Johnson et al. (1993). A precision of 1–2 μmol/kg was determined by the analysis of reference material (CRM, produced and distributed by A. Dickson, Scripps Institution of Oceanography). Data for concentrations of chlorophyll *a*, Chl, were available at intervals of 30–60 nautical miles during both cruises.

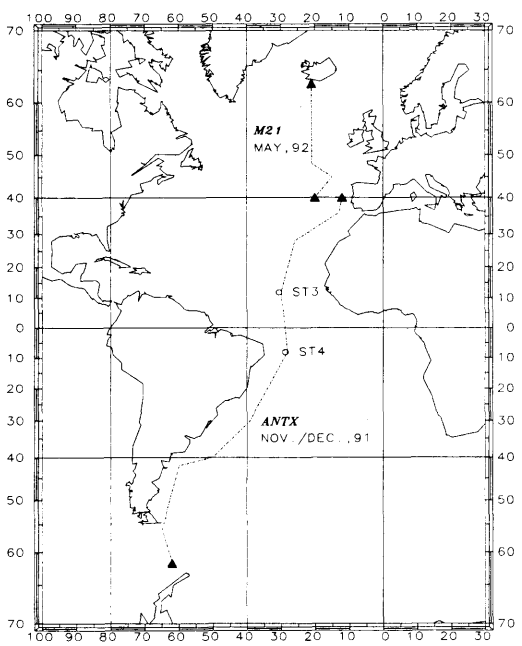

Fig. 1. Transects and stations during the cruise ANTX/1 in November/December 1991 with R. V. POLARSTERN and during the cruise M21 in May 1992 with R. V. METEOR.

3. CO_2 in the atmosphere

The CO_2 contents in the atmosphere (Fig. 2) are given as volume mixing ratios (ppm) in dry air. The data from the cruise ANTX/1 are used to estimate the north/south gradient between 40°N and 60°S. A decrease of 0.026 ppm per degree latitude was calculated. This corresponds to a difference of 2.6 ppm between 40°N and 60°S and is in agreement with the mean trend of the data from the NOAA/GMCC flask network (Tans et al., 1990). The data from the M21 cruise do not allow the determination of a gradient and therefore a mean value is calculated for the area 40°N–60°N, which is 359.5 ppm. Watson et al. (1991) report an atmospheric CO_2 content for May 1989 in the same area of 355.0 ppm. Hence, a mean growth rate of 1.5 ppm/y is obtained. This is somewhat higher than the mean global growth rate of

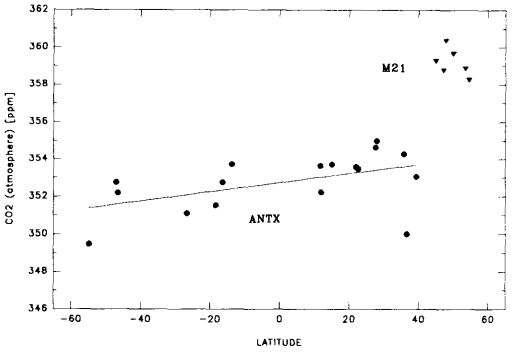

Fig. 2. Distribution of CO_2 mixing ratios in dry air over the Atlantic Ocean during ANTX/1 (November/December 1991) and M21 (May 1992).

1.22 ppm/y during 1981–1984 (Conway et al., 1988), but within the range of growth rates measured at individual stations (Boden et al., 1990).

The offset between the mean CO_2 content during the M21 cruise and the value at 40° N for the ANTX/1 cruise is 5.7 ppm and is attributed to the time shift between the measurements from May to November. The difference is consistent with a seasonal peak-to-peak amplitude for the North Atlantic of 10–14 ppm with a maximum in April and a minimum in September (Conway et al., 1988).

4. CO_2 in surface water

Profiles for $(pCO_2)_{sw}$ and $(pCO_2)_{atm}$ between Iceland and the Antarctic Peninsula are shown in Fig. 3a. Data points for $(pCO_2)_{sw}$ represent averages over 0.1° latitude. The $(pCO_2)_{atm}$ is obtained from CO_2 mixing ratios by multiplication with the barometric pressure reduced by the water vapour pressure at sea surface temperature. For 40° N–63° N a mean mixing ratio is used, whereas for 62° S–40° N the mixing ratios are calculated from the regression line in Fig. 2.

The differences between the $(pCO_2)_{sw}$ and the $(pCO_2)_{atm}$ curve (Fig. 3a) indicate that for the time of the measurements and at the longitude of the investigations, the surface waters of the Atlantic Ocean are mainly undersaturated with respect to CO_2.

Lowest partial pressure differences (–100 μatm) are found over the South American shelf area between 45° S and 55° S, but also under open

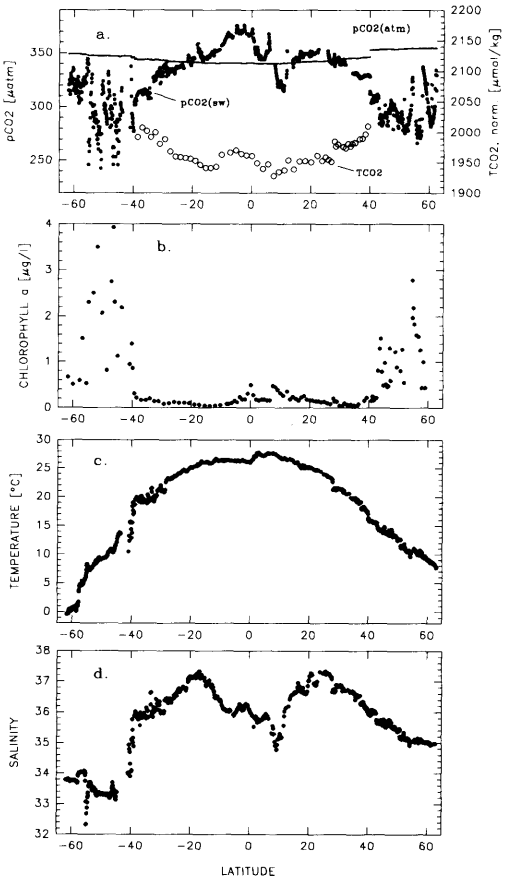

Fig. 3. Distribution of $(pCO_2)_{sw}$, $(pCO_2)_{atm}$, normalized ($S = 35°/_{oo}$) TCO_2 (a), chlorophyll *a* (b), temperature (c), and salinity (d) in the Atlantic Ocean during ANTX/1 and M21. For $(pCO_2)_{sw}$, temperature and salinity, averages over 0.1° latitude are presented.

ocean conditions, low partial pressure differences (–80 μatm) are observed at high latitudes in the north. A significant oversaturation exists only between the equator and 10° S with a relatively modest ΔpCO_2 maximum of 35 μatm. A quantitative comparison of our latitudinal ΔpCO_2 distribution with similar investigations in the Atlantic Ocean, but in other regions at different times, (e.g., Takahashi, 1961; Büchen, 1971; Roos and Gravenhorst, 1984) is extremely difficult, as ΔpCO_2 does not only depend on latitude, but also on longitude and, especially at higher latitudes, on the season (Takahashi et al., 1993).

The $(pCO_2)_{sw}$ profile (Fig. 3a) shows a certain interhemispheric symmetry with a peak in $(pCO_2)_{sw}$ of 375 μatm close to the equator and low values of 250 μatm and 270 μatm at high latitudes in the southern and northern hemisphere, respectively. A reverse regularity is observed for TCO_2 which was normalized to a salinity of 35 $^{o}/_{oo}$ in order to remove the effect of dilution by precipitation or concentration enhancement by evaporation. The normalized TCO_2 is lowest close to the equator and increasing towards higher latitudes (Fig. 3a). These large-scale distribution patterns correspond to an approximate interhemispheric symmetry also for temperature, salinity and the abundance of chlorophyll *a* (Fig. 3b–d), which are properties that (T, S) either act directly on $(pCO_2)_{sw}$ or, in the case of Chl, indicate the effect of photosynthesis on $(pCO_2)_{sw}$. Therefore, an attempt is made to relate these parameters to $(pCO_2)_{sw}$.

4.1. $(pCO_2)_{sw}$ at high latitudes ($>40°$)

The investigations in these areas were performed during May in the north and during December in the south and hence reflect spring time conditions in both hemispheres. The levels of Chl are clearly elevated (Fig. 3b) as a consequence of enhanced primary production especially over the South American shelf area and the $(pCO_2)_{sw}$ is characterized by an extremely high variability (Fig. 3a). A plot of $(pCO_2)_{sw}$ versus Chl and corresponding regression lines calculated separately for the data from the southern and the northern hemispheres (Fig. 4) show a distinct correlation and indicate that biological production is an important control for $(pCO_2)_{sw}$ during spring at high latitudes. The slopes of the two regression lines are quite similar, -18 μatm/(μg/l) and -13 μatm/(μg/l) for the southern and northern hemisphere, respectively. But the scatter of the data points around the regression lines is considerable and may be explained by the fact, that Chl is a questionable parameter for quantification of biological activity on $(pCO_2)_{sw}$. Ideally, such a parameter should represent the integrated net conversion of inorganic into organic carbon with respect to a reference time, e.g., the start of a spring bloom. However, Chl represents only a fraction of the total organic carbon production, a fraction which is varying with time due to sedimentation and changing composition of the biomass. Hence, we cannot expect a strong correlation between $(pCO_2)_{sw}$ and Chl. Nevertheless, the observed relationship gives a qualitative indication of the importance of biological production for $(pCO_2)_{sw}$. These conclusions are consistent with findings of Watson et al. (1991) who report $d(pCO_2)_{sw}/dChl$ values obtained from spring measurements between 47° N and 60° N at 20° W which vary in dependence on the state of the plankton bloom between -6.6 μatm/(μg/l) and -16.8 μatm/(μg/l).

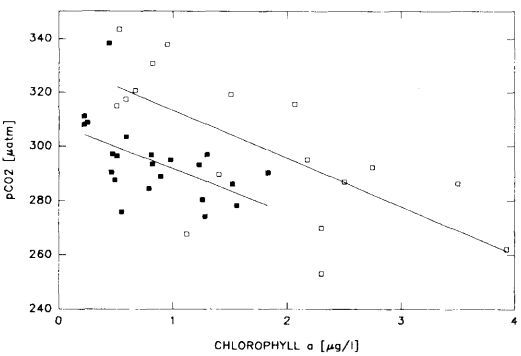

Fig. 4. Correlation between $(pCO_2)_{sw}$ and chlorophyll *a* at latitudes >40° in the southern (□) and northern (■) hemisphere.

The influence of temperature on the $(pCO_2)_{sw}$ distribution at high latitudes was also examined. Plots of $(pCO_2)_{sw}$ versus T for high latitudes are given in Fig. 5. No relationship is detectable in the south in spite of a strong temperature gradient between 40° S–62° S (Fig. 3c). The expected thermodynamical effect of increasing $(pCO_2)_{sw}$ with increasing T is masked by the strong influence of biological production. For the temperature range 6°C–9°C, the relationship is even reversed, because higher temperatures reflect the formation of a flat mixed layer which favours the development of a plankton bloom. Similar relationships are reported by Watson et al. (1991) for the Northeast Atlantic.

Also in the north, no uniform trend of $(pCO_2)_{sw}$ with T is observed (Fig. 5). Only for temperatures greater than 12°C, which refer to relatively low Chl values of about 1 μg/l (Fig. 3b, c) a weak correlation between $(pCO_2)_{sw}$ and T appears. In this area between 40° N–51° N the plankton bloom has possibly reached its senescent stage and the temperature control of the $(pCO_2)_{sw}$ distribution gains importance.

An effect of salinity on the distribution of $(pCO_2)_{sw}$ at high latitudes could not be identified.

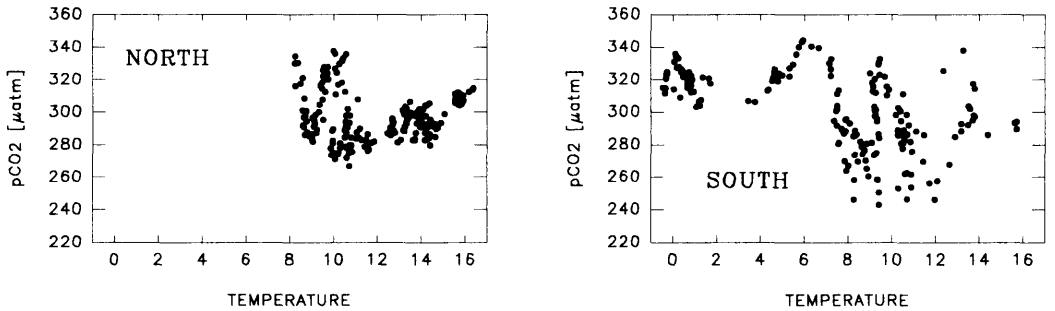

Fig. 5. CO_2 partial pressure as a function of temperature at latitudes >40°.

4.2. $(pCO_2)_{sw}$ at low latitudes, 40°S–40°N

The investigations in this region were performed during ANTX/1 in November/December. Conditions differ from that at high latitudes mainly because of strongly reduced concentrations of chlorophyll *a* (Fig. 3b). This indicates low biological activity and the distribution of $(pCO_2)_{sw}$ is mainly controlled by other processes. To examine the effect of temperature, a plot of $(pCO_2)_{sw}$ versus T is given in Fig. 6. Three different regimes may be distinguished. The regions between 16°N–40°N and 17°S–40°S, where a distinct correlation between $(pCO_2)_{sw}$ and temperature is found, and the tropical area between 17°S–16°N, where no relationship between $(pCO_2)_{sw}$ and T is detectable.

The fit of a straight line to the data north and south of the tropics gives a slope of 3.1 µatm/°C and 4.9 µatm/°C, respectively. This corresponds to a 0.9% and 1.5% increase in $(pCO_2)_{sw}$ per °C, respectively. Assuming that no exchange with the atmosphere occurs during temperature changes of surface water (TCO_2 = const.), a temperature coefficient of about 4.2%/°C is predicted by the thermodynamics of the carbonate system and empirical investigations (Gordon and Jones, 1973). The observed values are by a factor 3–4 lower and indicate that temperature changes in the investigated areas are slow and that the exchange with the atmosphere almost compensates changes of $(pCO_2)_{sw}$. Takahashi et al. (1993) present $(pCO_2)_{sw}$ data for the South Atlantic which also show a clear relationship to temperature for T > 16°C. However, using their data we estimated a temperature coefficient of about 2.5%/°C which is considerably higher than the value derived from our data (1.5%/°C). This discrepancy may be explained by the fact that the data reported by Takahashi et al. (1993) refer to different seasons and cover all longitudes between the South American and South African coast and therefore represent an annual mean for the South Atlantic north of about 40° S.

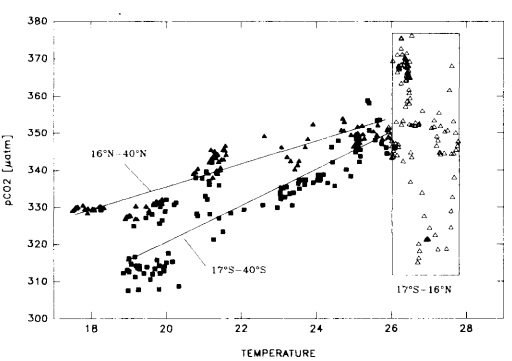

Fig. 6. CO_2 partial pressure as a function of temperature at latitudes between 40° S and 40° N.

For other parts of the world ocean, values between 1.2%/°C and 4.3%/°C are reported and were used to extrapolate $(pCO_2)_{sw}$ data into areas where data were not available (Tans et al., 1990). However, applying this approach, one should keep in mind that temperature coefficients highly depend on the dynamic conditions in the various hydrographic regimes and also show a seasonal variation (Takahashi et al., 1993; Poisson et al., 1993). Moreover, an empirical relationship between $(pCO_2)_{sw}$ and temperature may be influenced by other processes that act on $(pCO_2)_{sw}$. In the case of our data, Fig. 7 shows that salinity is correlated with temperature in the area where a correlation

Tellus B/47/1/2-7

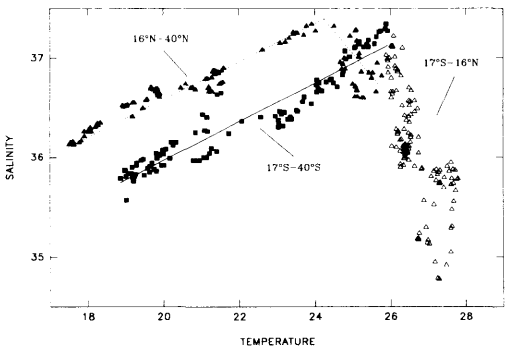

Fig. 7. Salinity/temperature diagram for 40° S–40° N.

between $(pCO_2)_{sw}$ and temperature was found. Hence, the empirical temperature coefficient includes also the effect of salinity on $(pCO_2)_{sw}$. A theoretical salinity coefficient ($TCO_2 = \text{const.}$), $d \ln(pCO_2)_{sw}/d S = 0.044$, corresponding to a 4.4% change per salinity unit, is calculated on the basis of the solubility constants (Weiss, 1974) and the equilibrium constants (Dickson and Millero, 1987). As this value is of the same magnitude as the temperature coefficient and as salinity increases by about 0.2 units per °C (Fig. 7), salinity accounts for about 20% of the observed temperature coefficients.

A correlation between $(pCO_2)_{sw}$ and T does not appear for the tropical area between 17° S and 16° N (Fig. 6), where temperature changes are low (<2°C), but where strong salinity gradients are observed (Fig. 7). Therefore, the relationship between $(pCO_2)_{sw}$ and salinity is examined. Fig. 8a gives a plot of $(pCO_2)_{sw}$ versus S for the region north of the salinity minimum (9.3° N–16° N). In spite of the few data, a distinct increase of $(pCO_2)_{sw}$ with increasing salinity is found and the corresponding coefficient $d \ln(pCO_2)_{sw}/d S$ amounts to $4.9\%/S$. This is slightly higher than the upper theoretical limit of $4.4\%/S$ for $TCO_2 = \text{const.}$ A simultanuous temperature increase which may intensify the salinity effect is not existent (Fig. 3c). But slightly elevated Chl values (Fig. 3b) are coinciding with the salinity minimum and are decreasing towards the north with increasing salinities. Thus, primary production contributes to a decrease of $(pCO_2)_{sw}$ at lower salinities and may explain the enhanced salinity coefficient.

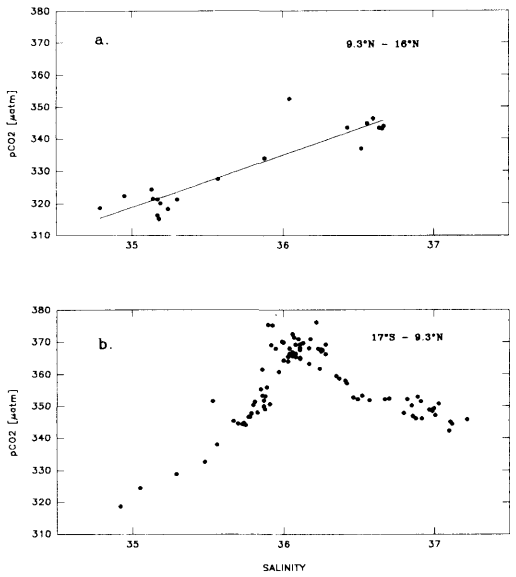

Fig. 8. CO_2 partial pressure as a function of salinity in the tropics: north of the salinity minimum (a) and south of the salinity minimum (b).

In the area south of the salinity minimum (9.3° N–17° S), salinity increases by more than two units from about $35\,^{o}/_{oo}$ to $37\,^{o}/_{oo}$, but the thermodynamical effect on $(pCO_2)_{sw}$ does not appear in the corresponding $(pCO_2)_{sw}/S$ plot (Fig. 8b). Instead, a $(pCO_2)_{sw}$ maximum is observed at salinities around $36.1\,^{o}/_{oo}$, which corresponds to latitudes between the equator and 10° S (Fig. 9a). This region is seperated from waters north of the equator by a drop in temperature of about 1.8°C (Fig. 9b). Simultanously, TCO_2 data, which are normalized to $S = 35\,^{o}/_{oo}$, show an elevated level between 0° S–10° S (Fig. 8c). From these observations we conclude that upwelling of cold CO_2-enriched water occurs and is responsible for the peak in $(pCO_2)_{sw}$. This conclusion is confirmed by the vertical profiles for T and TCO_2 (Fig. 10) at stations 3 and 4 (Fig. 1). Station 3 (12° N) is located close to the salinity minimum. A surface mixed layer of about 30 m is clearly separated from underlying water by strong gradients of temperature and TCO_2. In contrast, at station 4 (8° S), which is located in the area of the $(pCO_2)_{sw}$ maximum, no distinct stratification is observed in the upper 200 m. The formation of a surface mixed layer is obviously inhibited by upwelling.

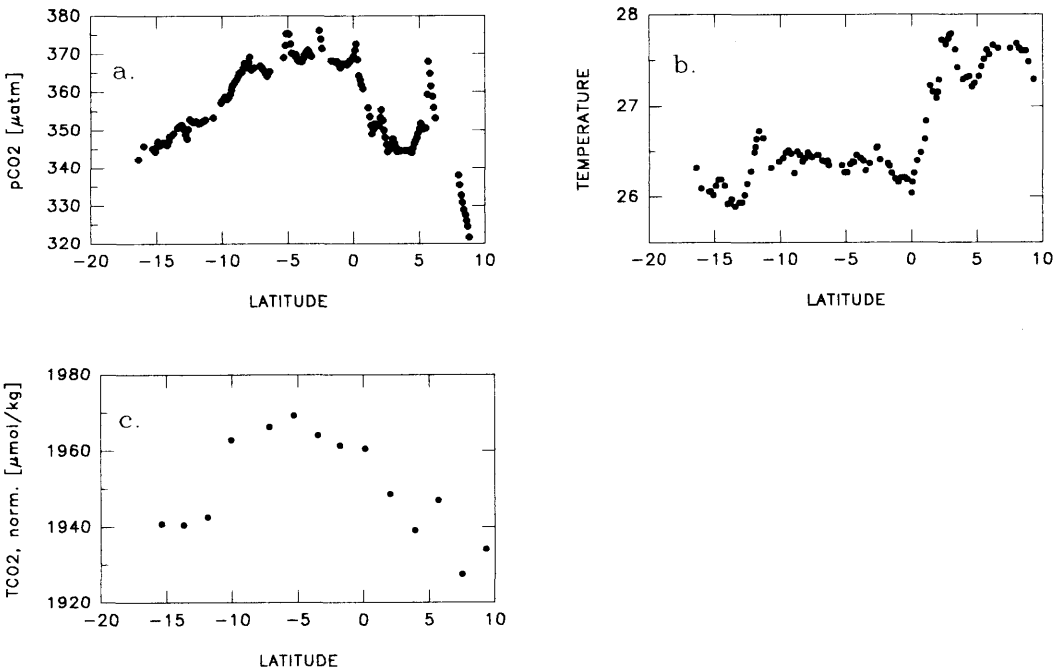

Fig. 9. $(pCO_2)_{sw}$ (a), temperature (b) and normalized ($S = 35‰$) TCO_2 (c) south of the tropical salinity minimum.

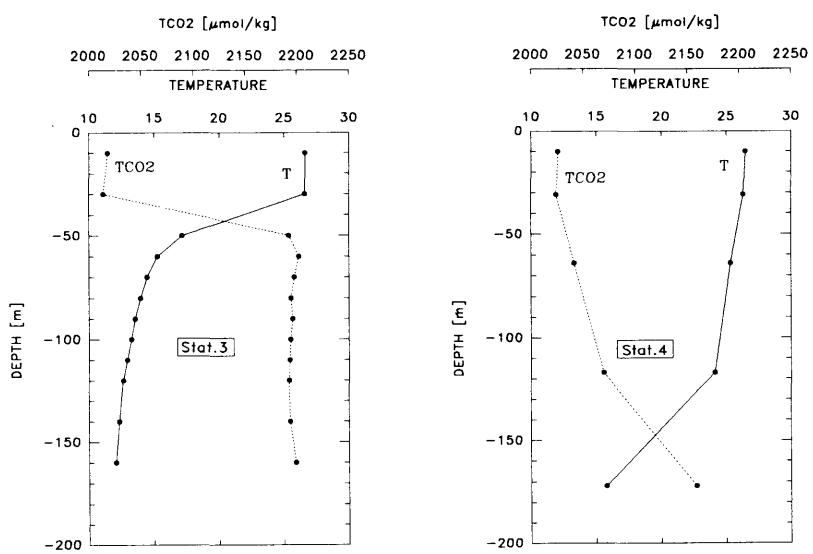

Fig. 10. Vertical distribution of temperature and TCO_2 in the upper 200 m at station 3 (12°N) and station 4 (8°S).

4.3. The Revelle factor

The distribution of TCO_2 in surface waters between 40° S–40° N (Fig. 3a) is thermodynamically linked to the distribution of $(pCO_2)_{sw}$ and may also be explained by an interplay of changes in temperature and salinity, production of biomass, upwelling and exchange with the atmosphere. To examine whether changes of $(pCO_2)_{sw}$ are thermodynamically consistent with changes of TCO_2, the Revelle factor is calculated, which is defined as the fractional change of $(pCO_2)_{sw}$ with the fractional change of TCO_2 at constant temperature, salinity and alkalinity:

$$[d(pCO_2)_{sw}/(pCO_2)_{sw}]/[d\ TCO_2/TCO_2] = R,$$

or

$$d \ln(pCO_2)_{sw}/d \ln TCO_2 = R.$$

To calculate R from field measurements, the effect of changing temperature and salinity on $(pCO_2)_{sw}$ and TCO_2 has to be eliminated. TCO_2 depends only on salinity and is normalized to $S = 35‰$, whereas $(pCO_2)_{sw}$ is a function of both, temperature and salinity. Normalization to $35‰$ and to a mean temperature of 23°C was performed in two steps. First, the alkalinity was calculated from the $(pCO_2)_{sw}$ and TCO_2 data on the basis of equilibrium constants given by Dickson and Millero (1987) and Weiss (1974). After that, the TCO_2 and calculated alkalinity data are normalized to $35‰$ and used to recalculate $(pCO_2)_{sw}$ at $35‰$ and 23°C. Fig. 11 shows $\ln pCO_2(35‰, 23°C)$ as a function of $\ln TCO_2(35‰)$. The slope of the regression line of 8.9 represents the mean Revelle factor for the investigated area and is typical for warm surface waters (Broecker and Peng, 1982). The scatter of the data points around the regression line reflects the wide temperature range (18°C–28°C) in the investigated area and changes in the specific alkalinity.

Takahashi et al. (1993) report Revelle factors of 11.36 and 10.97, which are based on $(pCO_2)_{sw}$ and TCO_2 data from four stations in the vicinity of Iceland and from 47° N/20° W, respectively. These values refer to lower mean temperatures, 5°C and 15°C, respectively, and therefore are not inconsistent with our value of 8.9 for 23°C.

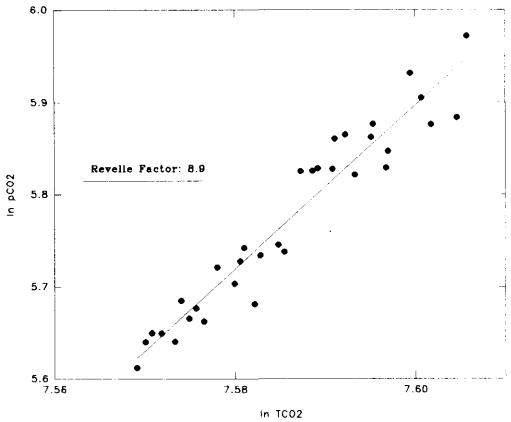

Fig. 11. Plot of $\ln(pCO_2)_{sw}$ (normalized to 23°C and $35‰$) versus TCO_2 (normalized to $35‰$) for the determination of the Revelle factor.

5. Conclusions

By the use of continuously recording underway systems $(pCO_2)_{sw}$ data with a high spatial resolution may be collected over vast areas. The $(pCO_2)_{sw}$ distribution pattern determined for the Atlantic Ocean between 62° S–63° N reflects a complex interplay of different processes that act on $(pCO_2)_{sw}$. Simple statistical methods may be applied to identify the processes which mainly control $(pCO_2)_{sw}$ in different regimes. In productive areas at the high latitudes a relationship between $(pCO_2)_{sw}$ and chlorophyll *a* concentrations indicate the dominating role of primary production. The subtropics are characterized by a correlation between $(pCO_2)_{sw}$ and temperature, but a salinity effect is superimposed to the temperature control of $(pCO_2)_{sw}$. For the tropics evidence was found that strong salinity gradients and upwelling determine the distribution of $(pCO_2)_{sw}$. Hence, correlation techniques are useful to explain $(pCO_2)_{sw}$ distributions on a qualitative basis. But the calculated regression coefficients $[d \ln(pCO_2)_{sw}/d\,T; d(pCO_2)_{sw}/d\,Chl]$ are only of limited regional and temporal importance and therefore we doubt, that they may be used to derive $(pCO_2)_{sw}$ fields by satellite observations of sea surface temperature and pigment distributions as discussed presently.

Along the investigated transects, the Atlantic Ocean appears mainly as a potential sink for atmospheric CO_2, a significant potential source

exists only in the narrow latitudinal band between the equator and 10°S, where upwelling occurs. This characteristic may change with time, especially at high latitudes, where the seasonality of temperature, biological production and depth of the mixed layer is substantial. But even for the time of our investigations, the observed latitudinal sink/source pattern is not representative for the Atlantic Ocean as a whole, because also longitudinal gradients have to be taken into account (Takahashi et al., 1993). Therefore, we do not present flux calculations and flux budgets, but consider our observations as a contribution to a comprehensive description of the seasonal and spatial ΔpCO_2 distribution in the Atlantic Ocean. However, this requires an international initiative to compile the growing amount of data, especially in the framework of JGOFS and WOCE, and to convert these into pCO_2 fields in a way proposed by Takahashi (1989).

6. Acknowledgements

We thank Ute Karbach, Peter Fritsche and Thomas Viergutz for their assistance in performing the pCO_2 measurements and chlorophyll analysis. Financial support for this work was provided by the German BMFT under grant number 03F0545A.

REFERENCES

Bacastow, R. B. and Maier-Reimer, E. 1990. Ocean-circulation model of the carbon cycle. *Clim. Dyn.* **4**, 95–125.

Boden, T. A., Kanciruk, P. and Farrell, M. P. 1990. *A compendium of data on global change.* ORNL/CDIAC-36, Oak Ridge National Laboratory, 257 pp.

Broecker, W. S. and Peng, T.-H. 1982. *Tracers in the sea.* Lamont Geological Observatory, Columbia University, Palisades, New York.

Büchen, M. 1971. Ergebnisse der CO_2-Konzentrationsbestimmung in der ozeannahen Luftschicht und im Oberflächenwasser während der atlantischen Expedition 1969. *"Meteor" Forschungserg.* **B37**, 55–70.

Conway, T. J., Tans, P., Waterman, L. S., Thoning, K. W., Masarie, K. A. and Gammon, R. H. 1988. Atmospheric carbon dioxide measurements in the remote global troposphere, 1981–1984. *Tellus* **40B**, 81–115.

Copin-Montegut, C. 1988. A new formula for the effect of temperature on partial pressure of CO_2 in seawater. *Mar. Chem.* **25**, 29–37.

Dickson, A. G. and Millero, F. J. 1987. A comparison of the equilibrium constants for the dissociation of carbonic acid in seawater media. *Deep-Sea Res.* **34**, 1733–1743.

Gordon, L. I. and Jones, L. B. 1973. The effect of temperature on carbon dioxide partial pressure in seawater. *Mar. Chem.* **1**, 317–322.

Johnson, K. M., Sieburth, J. McN., Williams, P. J. le B. and Brandstrom, L. 1987. Coulometric total carbon dioxide analysis for marine studies: Automation and calibration. *Mar. Chem.* **21**, 117–133.

Johnson, K. M., Wills, K. D., Butler, D. B., Johnson, W. K. and Wong, C. S. 1993. Coulometric total carbon dioxide analysis for marine studies: Maximizing the performance of an automated gas extraction system and coulometric detector. *Mar. Chem.* **44**, 167–187.

Keeling, C. D., Piper, S. C. and Heimann, M. 1989. A three-dimensional model of atmospheric CO_2 transport based on observed winds (4). Mean annual gradients and interannual variations. In: "Aspects of climate variability in the Pacific and the western Americas", D. H. Peterson (ed.). *AGU Geophys. Monogr.* **55**, 305–363.

Orr, J. C. 1993. Accord between ocean models predicting uptake of anthropogenic CO_2. *Water, Air & Soil Pollution* **70**, 465–481.

Poisson, A., Metzl, N., Brunet, C., Schauer, B., Bres, B., Ruiz-Pino, D. and Louanchi, F. 1993. Variability of sources and sinks of CO_2 in the Western Indian and Southern Oceans during the year 1991. *J. Geophys. Res.* **98**, No. C12, 22759–22778.

Roos, M. and Gravenhorst, G. 1984. The increase in oceanic carbon dioxide and the net CO_2 flux into the North Atlantic. *J. Geophys. Res.* **89**, 8181–8193.

Sarmiento, J. L. and Sundquist, E. 1992. Oceanic uptake of anthropogenic CO_2: a new budget. *Nature* **356**, 589–593.

Schneider, B., Kremling, K. and Duinker, J. C. 1992. CO_2 partial pressure in northeast Atlantic and adjacent shelf waters: Processes and seasonal variability. *J. Mar. Syst.* **3**, 453–463.

Takahashi, T. 1961. Carbon dioxide in the atmosphere and in Atlantic Ocean water. *J. Geophys. Res.* **66**, 477–494.

Takahashi, T. 1989. Only half as much CO_2 as expected from industrial emissions is accumulating in the atmosphere. Could the oceans be the storehouse for the missing gas? *Oceanus* **32**, 22–29.

Takahashi, T., Olafsson, J., Goddard, J. G., Chipman, D. W. and Sutherland, S. C. 1993. Seasonal variation of CO_2 and nutrient salts in the high latitude oceans: a comparative study. *Global Biogeochem. Cycles* **7**, 843–848.

Tans, P., Fung, Y. and Takahashi, T. 1990. Observational constraints on the global CO_2 budget. *Science* **247**, 1431–1438.

Watson, A. J., Robinson, C., Robertson, J. E., Williams, P. J. le B. and Fasham, M. J. R. 1991. Spatial variability in the sink for carbon dioxide in the North Atlantic. *Nature* **350**, 50–53.

Watson, R. T., Meira Filho, L. G., Sanhueza, E. and Janetos, A. 1992. In: *Climate change 1992:* The Supplementary Report to the IPCC Scientific Assessment, J. T. Houghton, B. A. Callander, S. K. Varney, (eds.). Cambridge Univ. Press, 1992, pp. 29–46.

Weiss, R. F. 1974. Carbon dioxide in water and seawater: The solubility of a non-ideal gas. *Mar. Chem.* **2**, 203–215.

Weiss, R. F., Jahnke, R. A. and Keeling, C. D. 1982. Seasonal effects of temperature and salinity on the partial pressure of CO_2 in seawater. *Nature* **300**, 511–513.